Electronic Supplementary Information

Vapour Solid Reaction Growth of SnO$_2$ Nanorods as an Anode Material for Li Ion Batteries

Kai-Chieh Hsu,[a] Chi-Young Lee,[b] and Hsin-Tien Chiu*[a]

[a]Department of Applied Chemistry, National Chiao Tung University, Hsinchu, Taiwan, 30010, R. O. C.

[b]Department of Materials Science and Engineering, National Tsing Hua University, Hsinchu, Taiwan, 30013, R. O. C.

*Corresponding author. E-mail: htchiu@nctu.edu.tw (H.-T. Chiu)

Table S1. Summary of electrochemical properties of Sn containing electrodes for rechargeable Li-ion batteries.

Table S2. Experimental conditions for samples prepared by reacting $SnCl_{4(g)}$ and $CaO_{(s)}$.

Figure S1. Low magnification SEM image in (a) shows the presence of a less observed morphology at the centre. (b) Enlarged view of the morphology.

Figure S2. (a) Low and (b) high magnification SEM images and (c) EDX data from an area of sample B. (d) – (f) Corresponding data from another area of B.

Figure S3. XRD patterns of samples B and C. Standard XRD patterns and the corresponding JCPDS file numbers are shown also.

Figure S4. Low and high magnification SEM images of samples D and E. The EDX data are from the selected areas marked by red rectangles. Images and EDX of D are shown in (a) – (c). The data suggest that D is composed of SnO_2. Images and EDX of E are shown in (d) – (h). There two types of solids. The NRs shown in (d) and (e) are SnO_2, indicated by the EDX result in (f). According to the EDX in (h), the particles in (g) are $CaSnO_3$. The assignments are consistent with the XRD results shown in Figure S5.

Figure S5. XRD patterns of samples A, D and E. Standard XRD patterns and the corresponding JCPDS file numbers are shown also.

Figure S6. (a) Discharge capacities of electrodes fabricated from commercial SnO_2 powders (sizes: 1 - 10 μm and 100 nm) at a cycling rate 100 mA g^{-1}. (b) Electrochemical performance of a SnO_2 NR electrode cycled between 0.005 V and 2.0 V vs. Li/Li$^+$ after first ten cycles were cycled at 100 mA g^{-1}. 100 mA g^{-1} (●), 500 mA g^{-1} (ɷ), 1000 mA g^{-1} (▢), and 3000 mA g^{-1} (❋).

Figure S7. (a) EDX of a SnO_2 NR electrode after 100 cycles of lithiation and de-lithiation. The upper result was obtained from the whole-scan of the area shown in Figure 4a. The Cl content was low. The Pt signal was from the sputtered Pt metal, used to enhance the sample conductivity. The lower result was from the centre–point of one NR. (b) XRD patterns of sample A before and after 100 cycles of lithiation and de-lithiation. Related XRD patterns and the corresponding JCPDS file numbers are shown also.

Figure S8. SEM image of an electrode fabricated from a mixture of commercial SnO_2 powder, carbon black, and binder after 50 cycles of lithiation and de-lithiation.

Table S1. Summary of electrochemical properties of Sn containing electrodes for rechargeable Li-ion batteries.

Electrode material	Experimental Method	Morphology and Composition	Electrochemical Performance			Ref
			Working Potential (V)	Cycling Rate	Capacity (mAh g^{-1})	
SnO_2 NTs NWs NPs	Sol–gel vacuum-suction Thermal-evaporation sol–gel	D of NT: 200 nm D, L of NW: 200 nm, ~tens μm Size of NP < 100 nm	0.05 – 1.5	50 cycles at 100 mA g^{-1} (1 C = 790 mA g^{-1})	250 210 90	14[a]
SnO_2 NTs	Infiltration technique	Diameter: 180 – 230 nm	0.005 – 2	80 cycles at 0.05 mA·cm^{-2}	525	15[b]
SnO_2 NWs	Thermal evaporation	Diameter: 200 – 500 nm Length: 10 μm	0.005 – 2.5	50 cycles at 100 mA g^{-1} (1 C = 782 mA g^{-1})	460	16[c]
SnO_2 nanoflowers	Free cation-induced decomposition	Diameter: 50 – 110 nm	0.01 – 2	20 cycles at 0.1 C (1 C = 783 mA g^{-1})	450	17[d]
SnO_2 nanosheets	Hydrothermal method	Thin: 1.5 – 3 nm	0.005 – 3	20 cycles at 0.1 C (1 C = 782 mA g^{-1})	559	18[e]
SnO_2 hollow nanospheres	Hydrothermal method	Diameter: 50 – 200 nm Wall thickness: 10 nm	0.005 – 2	40 cycles at 0.2 C (1 C = 645 mA g^{-1})	450	19[f]
SnO_2 NRs	Vapour-Solid Reaction Growth (VSRG)	Diameter: 15 nm, Length: 1000 nm	0.005 – 2	100 cycles at 100 mA g^{-1} (1 C = 790 mA g^{-1})	435	This work

| SnO$_2$/Cu nanosheets | Rolled-up nanotechnology | SnO$_2$ film: 50 nm, Cu film: 3 nm | 0.05 – 1.5 | 150 cycles at 100 mA g^{-1} (1 C = 782 mA g^{-1}) | 764 | 36[g] |

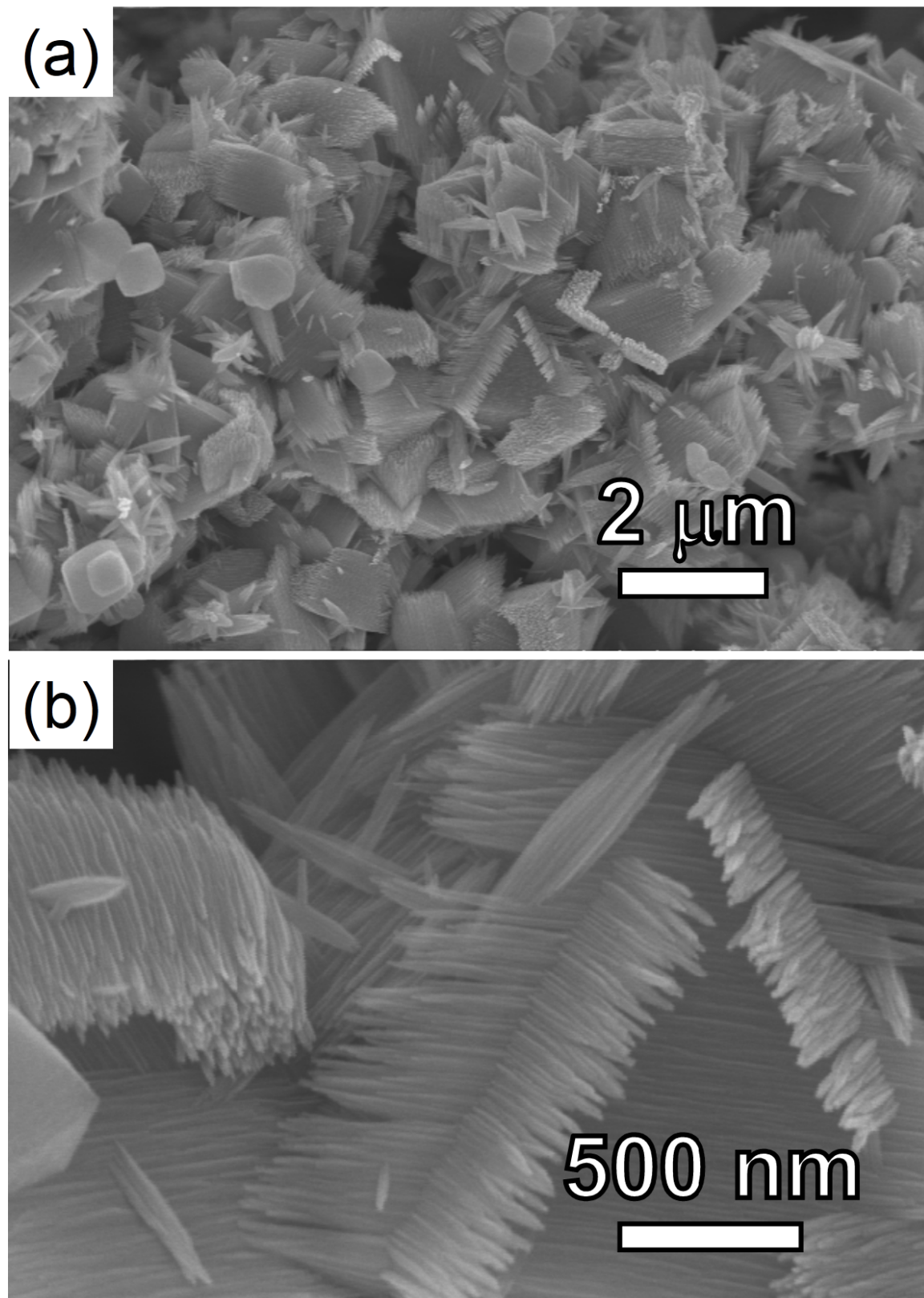NT: nanotube, NW: nanowire, NP: nanoparticle.

a. M.-S. Park, Y.-M. Kang, G.-X. Wang, S.-X. Dou and H.-K. Liu, *Adv. Funct. Mater.*, 2008, **18**, 455-461.

b. Y. Wang, J. Y. Lee and H. C. Zeng, *Chem. Mater.*, 2005, **17**, 3899-3903.

c. M. S. Park, G. X. Wang, Y. M. Kang, D. Wexler, S. X. Dou and H. K. Liu, *Angew. Chem.*, 2007, **119**, 764-767.

d. J. Ning, Q. Dai, T. Jiang, K. Men, D. Liu, N. Xiao, C. Li, D. Li, B. Liu, B. Zou, G. Zou and W. W. Yu, *Langmuir*, 2009, **25**, 1818-1821.

e. C. Wang, Y. Zhou, M. Ge, X. Xu, Z. Zhang and J. Z. Jiang, *J. Am. Chem. Soc.*, 2010, **132**, 46-47.

f. X. W. Lou, Y. Wang, C. Yuan, J. Y. Lee and L. A. Archer, *Adv. Mater.*, 2006, **18**, 2325-2329.

g. J. Deng, C. Yan, L. Yang, S. Baunack, S. Oswald, H. Wendrock, Y. Mei and O. G. Schmidt, *ACS Nano*, 2013, **7**, 6948-6954.
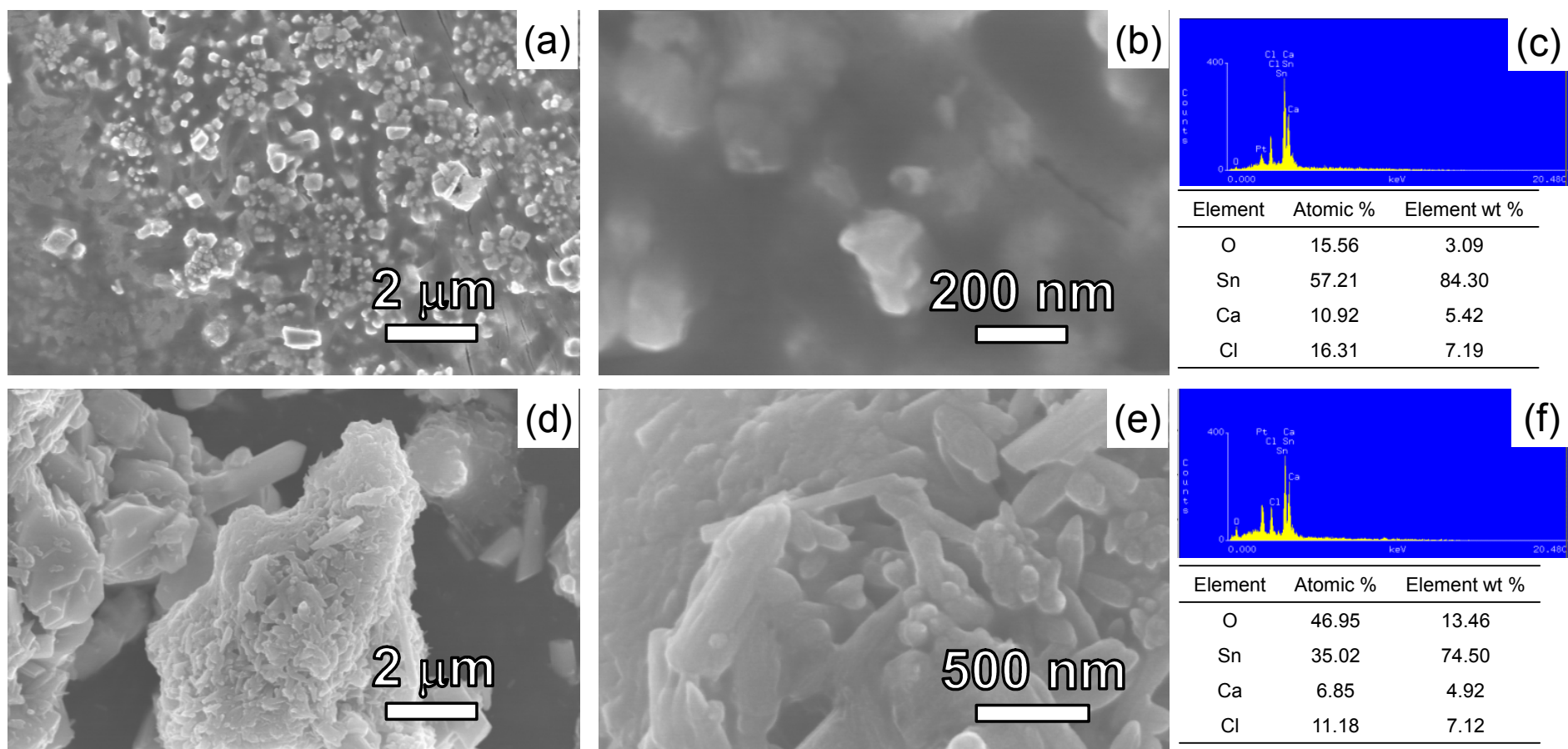
Table S2. Experimental conditions for samples prepared by reacting $SnCl_{4(g)}$ and $CaO_{(s)}$.

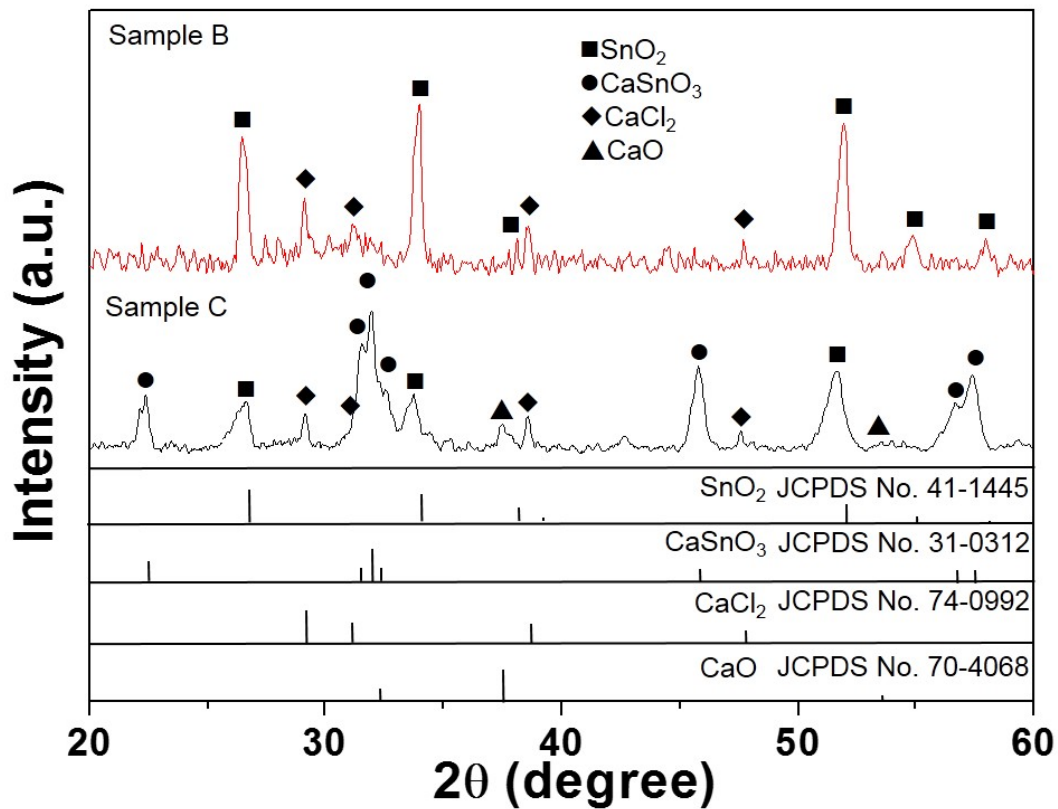| Sample	Reaction Temperature (K)	Reaction Time (min)	Washed by $H_2O_{(l)}$	Observed Solid Phases in the Product
A	1023	360	Yes	$SnO_{2(s)}$
B	1023	360	No	$SnO_{2(s)}$, $CaCl_{2(s)}$
C	1023	60	No	$SnO_{2(s)}$, $CaSnO_{3(s)}$, $CaCl_{2(s)}$, $CaO_{(s)}$
D	1073	360	Yes	$SnO_{2(s)}$
E	973	360	Yes	$SnO_{2(s)}$, $CaSnO_{3(s)}$

$SnCl_{4(l)}$ was evaporated at room temperature by $Ar_{(g)}$ (10 sccm). Another flowing stream of $Ar_{(s)}$ (10 sccm) was also introduced into the reactor.

Figure S1.   Low magnification SEM image in (a) shows the presence of a less observed morphology at the centre. (b) Enlarged view of the morphology.
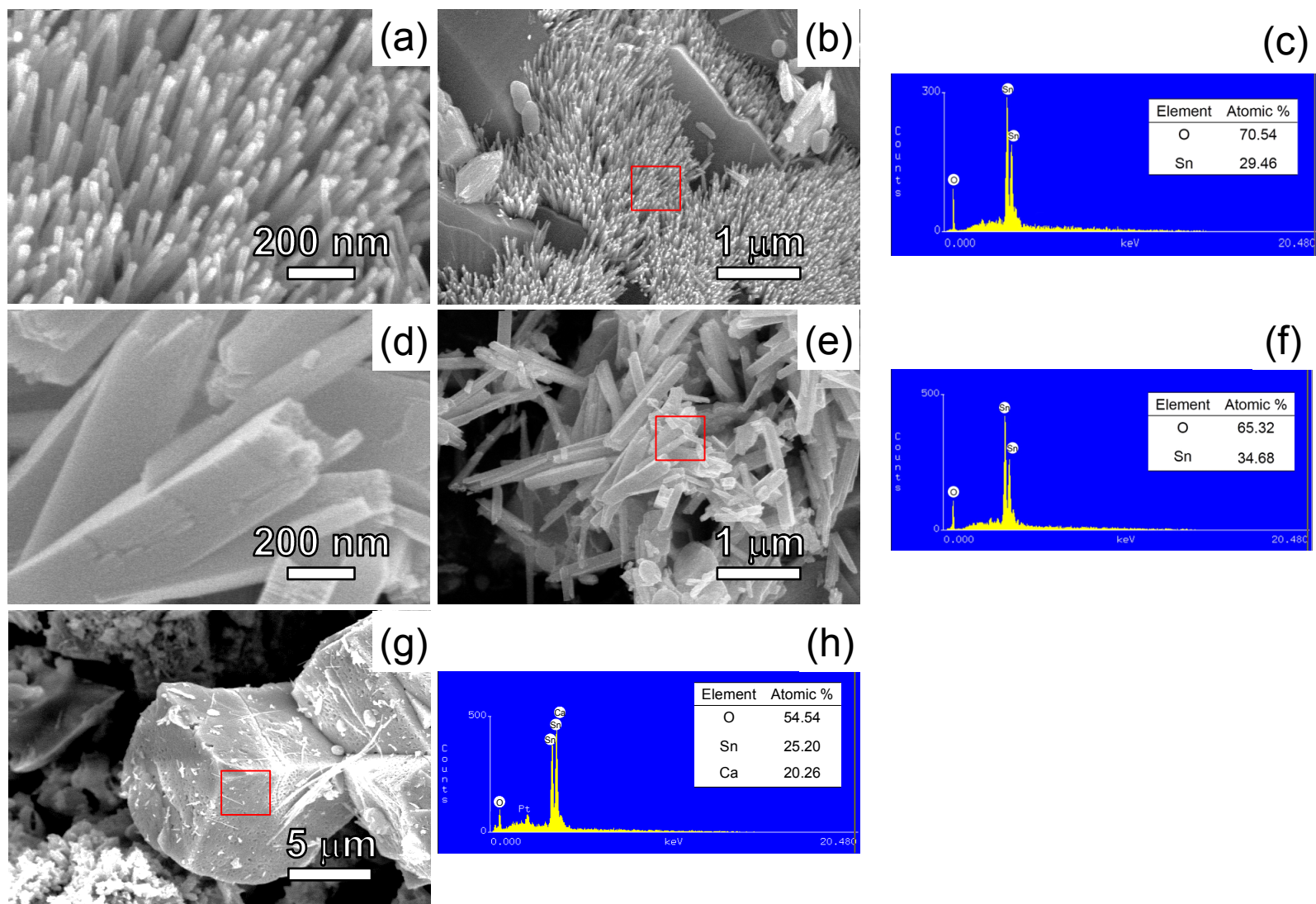
Element	Atomic %	Element wt %
O	15.56	3.09
Sn	57.21	84.30
Ca	10.92	5.42
Cl	16.31	7.19

Element	Atomic %	Element wt %
O	46.95	13.46
Sn	35.02	74.50
Ca	6.85	4.92
Cl	11.18	7.12

Figure S2. (a) Low and (b) high magnification SEM images and (c) EDX data from an area of sample B. (d) – (f) Corresponding data from another area of B.
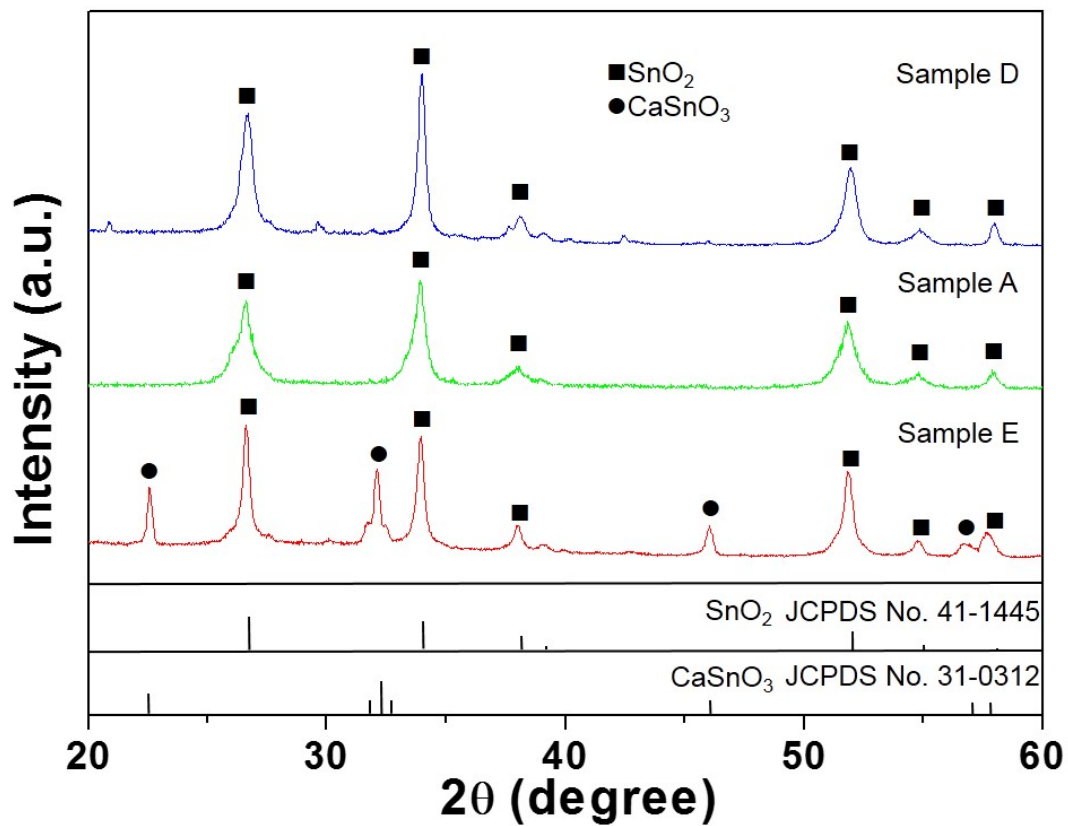
Figure S3.   XRD patterns of samples B and C. Standard XRD patterns and the corresponding JCPDS file numbers are shown also.
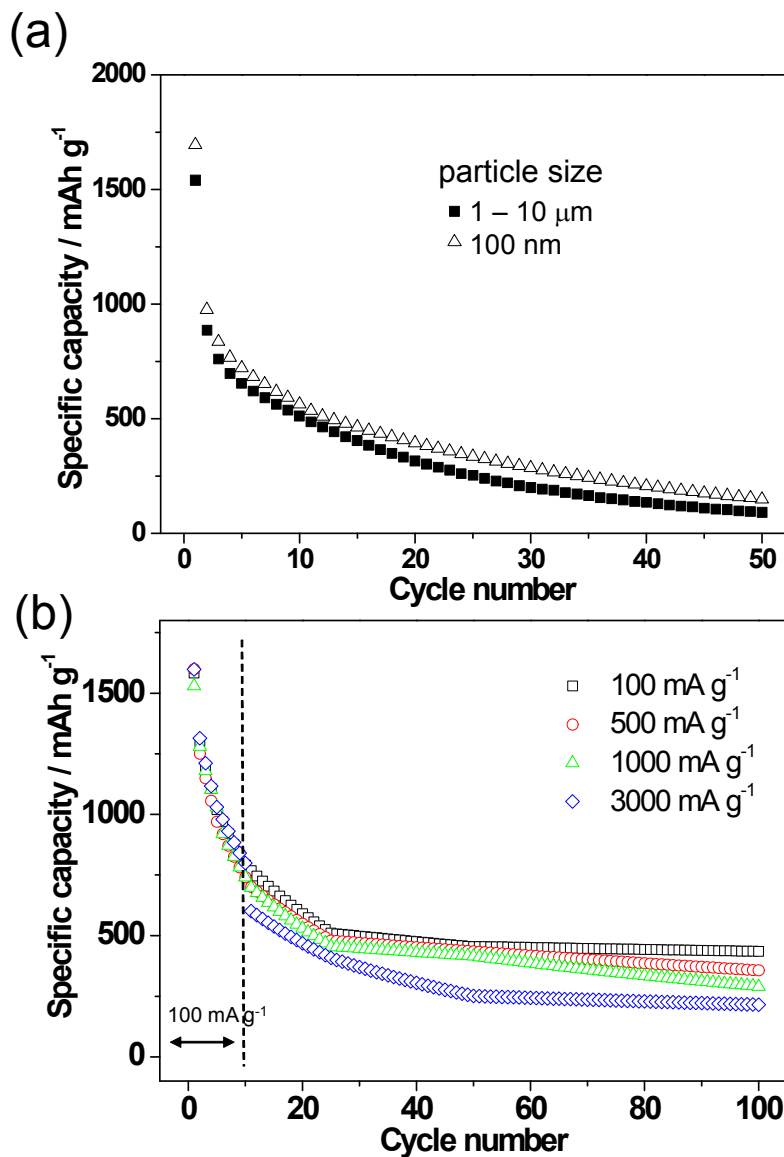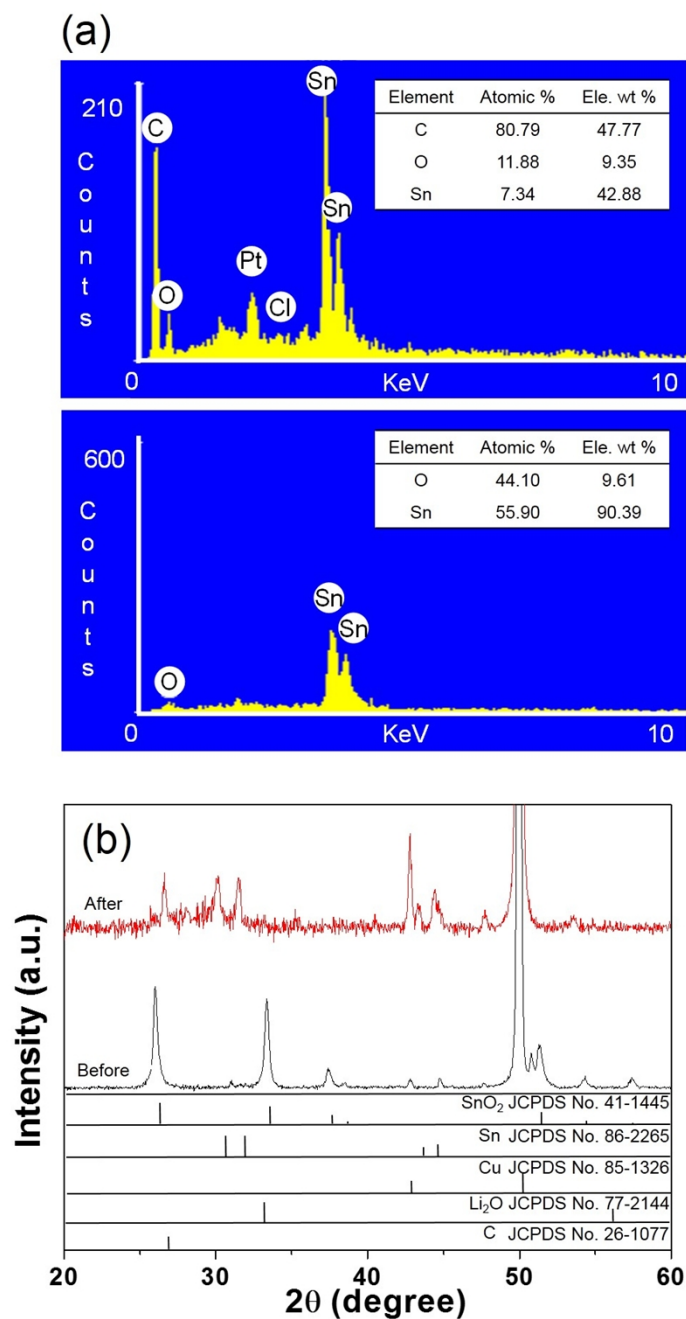
Figure S4. Low and high magnification SEM images of samples D and E. The EDX data are from the selected areas marked by red rectangles. Images and EDX of D are shown in (a) – (c). The data suggest that D is composed of SnO_2. Images and EDX of E are shown in (d) – (h). There two types of solids. The NRs shown in (d) and (e) are SnO_2, indicated by the EDX result in (f). According to the EDX in (h), the particles in (g) are $CaSnO_3$. The assignments are consistent with the XRD results shown in Figure S5.
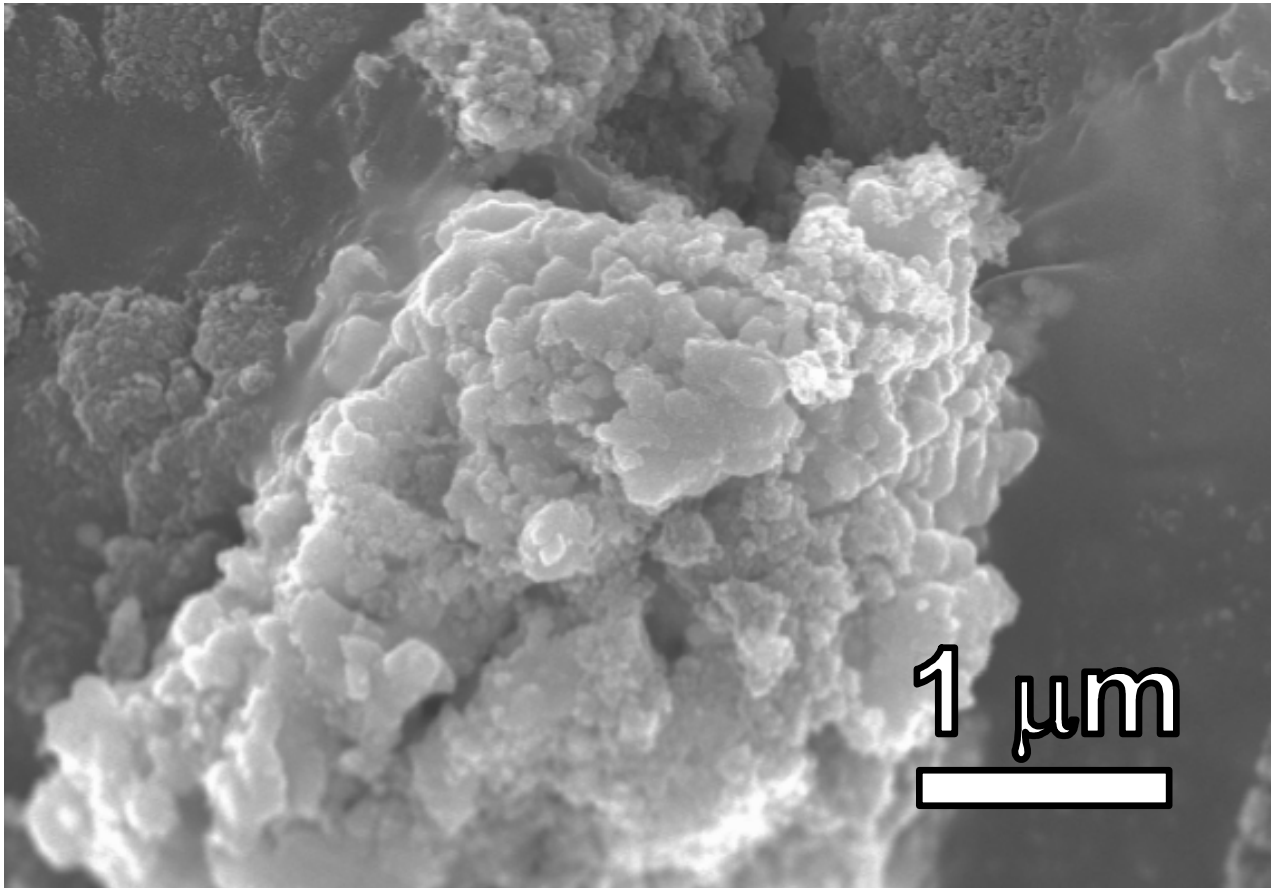
Figure S5. XRD patterns of samples A, D and E. Standard XRD patterns and the corresponding JCPDS file numbers are shown also.

Figure S6. (a) Discharge capacities of electrodes fabricated from commercial SnO_2 powders (sizes: 1 - 10 μm and 100 nm) at a cycling rate 100 mA g^{-1}. (b) Electrochemical performance of a SnO_2 NR electrode cycled between 0.005 V and 2.0 V vs. Li/Li$^+$ after first ten cycles were cycled at 100 mA g^{-1}. 100 mA g^{-1} (●), 500 mA g^{-1} (∝), 1000 mA g^{-1} (◻), and 3000 mA g^{-1} (❋).

Figure S7. (a) EDX of a SnO$_2$ NR electrode after 100 cycles of lithiation and de-lithiation. The upper result was obtained from the whole-scan of the area shown in Figure 4a. The Cl content was low. The Pt signal was from the sputtered Pt metal, used to enhance the sample conductivity. The lower result was from the centre–point of one NR. (b) XRD patterns of sample A before and after 100 cycles of lithiation and de-lithiation. Related XRD patterns and the corresponding JCPDS file numbers are shown also.

Figure S8.   SEM image of an electrode fabricated from a mixture of commercial SnO$_2$ powder, carbon black, and binder after 50 cycles of lithiation and de-lithiation.